3 – Experimental Methods

3.1 Deposition methods

3.1.1 Radio Frequency Plasma Enhanced Chemical Vapour Deposition (RFCVD)

The reactor used in this study is a converted parallel plate reactive ion etching system. A schematic diagram can be seen in Figure 3.1. The system consists of two circular electrodes. The powered electrode in the centre is where the substrate is placed for deposition. The rest of the inside of the reaction chamber is earthed and the top of this forms the grounded electrode.

The RF-power is supplied by a 13.56 MHz power supply. To maximise forward power and to minimise reverse power (which can damage the power supply), the RF power is fed through a set of variable capacitors and an inductor before being connected to the chamber. Upon striking a plasma these variable capacitors had to be adjusted manually to minimise reverse power.

The DC-Bias and (V_{DC}) and the peak-to-peak voltage were measured via a set of resistors connected to the electrodes. These resistors decreased the bias and peak-to-peak voltages (typically hundreds of V) to safely measurable voltages (typically 0-5 V). These voltages were read using a digital voltage meter (DVM).

Vacuum is maintained via a two stage rotary vacuum pump (Edwards two-stage 90), which can be isolated by means of a pneumatic poppet valve. The chamber vacuum is measured via a “Baratron” capacitance manometer vacuum gauge; the gauge reads

between 0.001-1.000 Torr. The base pressure of the deposition system is below 0.001 Torr.

Source gases are admitted to the chamber from the shower head in the grounded electrode. The flow rate and gas mixture were controlled by calibrated mass flow controllers (MFC). Two sets of MFCs are connected to the apparatus. The first set allows deposition gases to be injected into the chamber. The deposition gases used in this study were methane (CH_4) and phosphine (PH_3). The gas cylinders from which these gases were supplied contained CP grade gas (supplied by BOC), the regulator pressures were kept at 25 PSI. The MFC for the CH_4 was a Millipore MFC. It had a maximum flow rate of 50 standard cubic centimetres per minute (SCCM). The MFC for PH_3 was a Millipore MFC. It had a maximum flow rate of 10 SCCM. The MFC had a Viton seal instead of a normal rubber one. This was due to the aggressive nature of the gas. Other precautions had to be taken to conduct experiments safely with PH_3. A nitrogen purge and pump down system was fitted to the high pressure side of the MFC, Figure 3.1 shows details of this. This meant that if the MFC stuck closed PH_3 could be removed safely. It also meant that PH_3 residues could be easily pumped away. After deposition, the PH_3 MFC was pumped down and the whole chamber was left for at least 15 minutes to pump down to base pressure to remove any toxic gases. When the chamber was vented, a custom designed fume extraction system was activated to allow any remaining toxic gases to be flushed away.

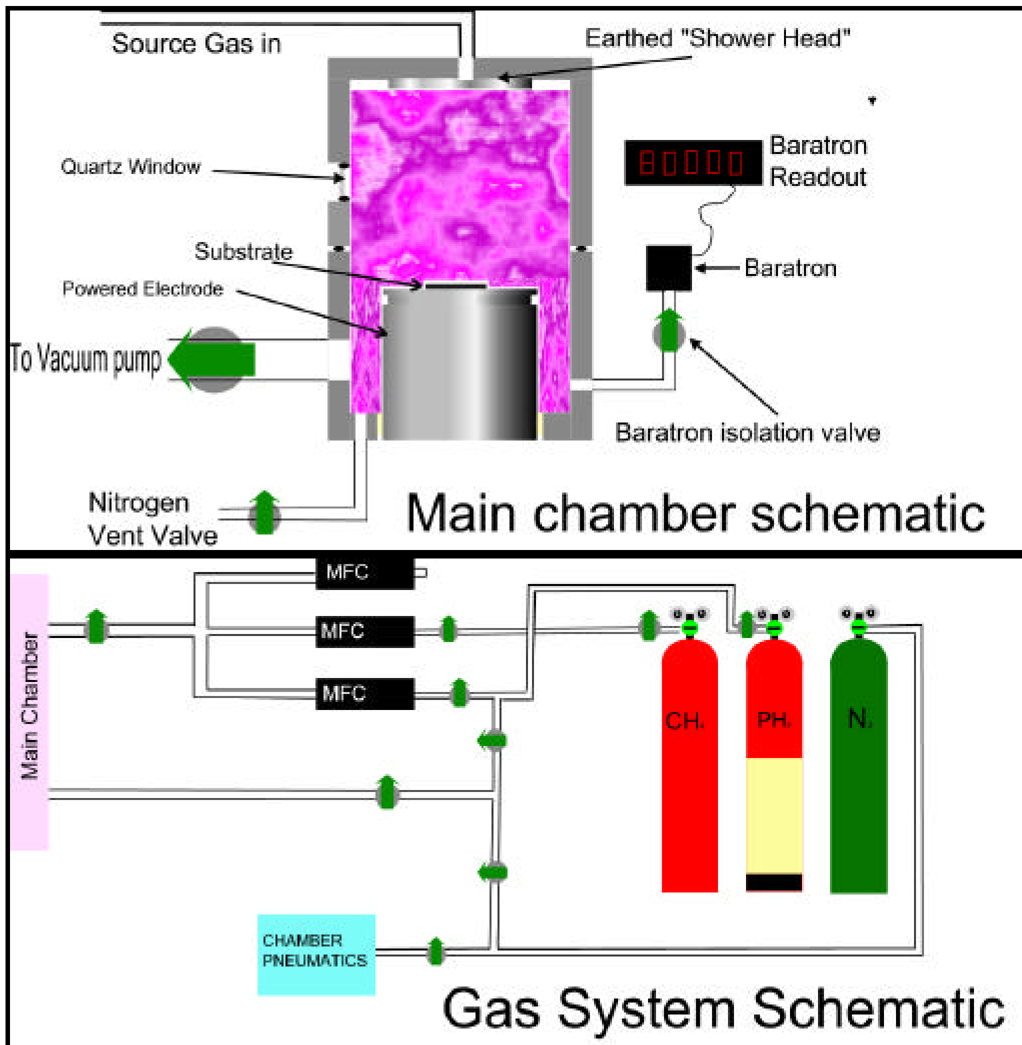

Figure 3.1: Schematic diagram and photographs of RF-CVD system.

The second set of MFCs allows air to be metered directly into the chamber so that an air plasma can be struck. This allows the chamber to be easily cleaned after manually removing most of the residue from deposition. An interlock with pneumatic valves prevented air from being bled into the system when the deposition gases were being used.

Three manual valves control the pressure, a rotary valve and two butterfly valves. These were necessary as fine control of the pressure was difficult and these valves helped to maintain a constant deposition pressure. Typical deposition pressures were between 10 – 40 mTorr.

The chamber was opened via a pneumatic hoist. All mechanical operations of the chamber are operated by dry nitrogen gas at around 35 PSI. The same nitrogen is used to vent the chamber.

B-doped Si 100 wafers, glass and quartz substrates were used during this study. Careful preparation and cleanliness were found to be essential to grow continuous films. Small amounts of contamination were found to cause film delamination. The substrates were cut to size (usually 1 cm^2). These were then soaked in isopropyl alcohol (IPA) and ultrasonically cleaned for 15 minutes. They were then carefully removed, dried in a stream of nitrogen, rinsed in IPA and dried under nitrogen again. They were then placed on the powered electrode and the reactor was pumped down without delay. One experiment was carried out with a fresh silicon surface prepared by rinsing the surface of the wafer with HF solution, under dry nitrogen.

To allow stabilisation of conditions within the chamber when pumped down to base pressure, the source gases were admitted for at least five minutes before the RF power

supply was switched on and the deposition pressure obtained. The power on the RF power supply was then wound up until the correct DC-bias was displayed on the DVM. Further adjustments of pressure and DC-bias were then necessary to obtain deposition conditions.

If stable conditions could not be obtained within 30 seconds of starting the RF power supply, the experiment was aborted, the substrates changed and the deposition restarted.

Throughout the experiment it was noticed that the DC-bias would decrease from the starting value. This was corrected by increasing the RF power. This effect was accounted for by the fact that an insulating coating was being grown all over the inside of the reactor, especially on the powered electrode. A previous study by Kuo *et al*[1] has attempted to quantify this effect. More details of why the deposition is preferential on the powered electrode and why this should affect the DC bias are available in chapter 2. Throughout deposition the DC-Bias was kept constant. This was done by adjusting the RF power.

Samples were then removed from the reactor and analysed or further processed as soon as possible after deposition. If analysis was not available immediately the samples were either kept in an evacuated desiccator, or stored under an inert gas such as nitrogen or argon.

Towards the end of this study a substrate heater was added to the apparatus. The heater allowed heating up to 260 ºC. This consisted of a cartridge heater placed within the powered electrode. Substrate temperature was measured via a thermocouple embedded in the powered electrode. Disconnecting the RF power

supply and attaching a cable connected directly to the heater operated it. The heater remained at a virtually constant temperature through deposition runs, as long as the runs were kept short (<10 minutes). The supply wires were changed for heating and deposition so that the RF power was not transmitted through the heater power supply wires.

3.1.2 Pulsed laser ablation at the solid-liquid interface (LP-PLA)

The deposition system used in this study is shown in Figure 3.2. The beam from a Nd:YAG laser (either the fundamental or 1st overtone) was steered by 90° by a prism and focused into the reaction vessel by a lens.

The laser used a frequency doubling crystal to obtain the 1st overtone (532 nm) beam from the fundamental (1064 nm) beam. The maximum power was 130 mJ per pulse for the 532 nm output and 450 mJ per pulse for the 1064 nm output. The pulse duration was 10 ns.

The beam was focused down to the smallest spot possible. This was done either by moving the lens up and down or by moving the reaction vessel up and down using a lab jack. A long focal length lens (25 cm) was used to prevent splashing of the lens by the liquid.

It is estimated that the focused laser spot had a diameter of approximately 0.02 cm. This corresponds to a maximum fluence of 414 $J\,cm^{-2}$ for 532 nm and 1432 $J\,cm^{-2}$ for 1064 nm.

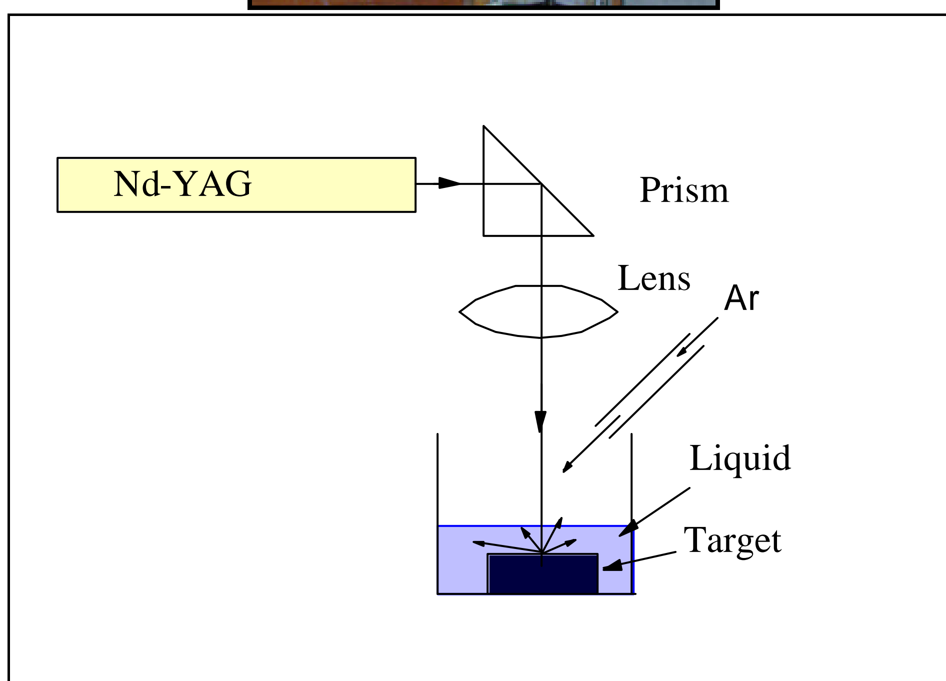

Figure 3.2: Photograph and schematic of Liquid/Solid interfaced pulsed laser ablation apparatus.

The reaction vessel had a solid target covering the bottom of the vessel. The solid target was red phosphorus, white phosphorus, graphite, or a graphite/red phosphorus mixture (the size of the solid target was not particularly important as the laser spot was small). The solid was covered in approximately 1 cm of liquid cyclohexane, xylene, acetone or water (depending on which deposition was being carried out).

A continuous argon stream was injected into the top of the reaction vessel if flammable liquids were being used, thus preventing fire.

For safety the system was enclosed in a black metal box. To allow observation of the reaction a piece of the metal box could be removed. Extra precautions had to be taken when using the 1064 nm beam. The lab had to be evacuated of anyone not wearing appropriate safety eyewear. This was because even a scattered beam from this invisible, high power light source could potentially cause blindness.

To deposit, the laser was focused onto the solid at the minimum spot size at a low power. The laser power was then increased to the required value. The reaction vessel was then observed and if necessary the liquid topped up every few minutes (topping up occurred more frequently when using 1064 nm). Deposition usually lasted for 15 minutes.

During deposition a loud cracking noise was heard from the reaction vessel. Light emission from the plume above the focal point was also observed, and recorded using OES.

Care had to be taken to make sure that the laser did not focus on the bottom of the reaction vessel. If this happened the bottom of the reaction vessel was quickly drilled through by the laser. To prevent this the amount of solid used was increased until it was unlikely that the beam would focus on the bottom of the reaction vessel, this was either by using large solid targets, or by using more smaller lumps of solid.

After deposition the liquid was pipetted off from the solid. These liquid samples were stored in air-tight vials. If there was an air gap in the top of the vial the sample was packed under argon.

3.1.2.1 Manufacture of Mixed Carbon/Phosphorus Targets for Laser Ablation at the Solid, Liquid Interface

Targets were manufactured by pressing mixtures of graphite powder and red phosphorus. A specialised powder press was used for this purpose. This press consisted of a hydraulic press and a stainless steel die and a rotary vacuum pump.

To manufacture a target the die was loaded with the powder and a stainless steel stub put on top of the powder. The die was then connected to the vacuum pump. The vacuum pump removed as much air as possible from the powder. The die was then placed in the hydraulic press and 8 tons of pressure was applied to the die for 30 seconds.

The targets that were produced were circular, with a diameter of 1 cm and approximately 1 mm in thickness.

3.2 Processing methods

3.2.1 Post Deposition Thermal Annealing

A hotplate was built to anneal samples. This consisted of a high vacuum chamber (base pressure $<10^{-7}$ Torr pumped by an Edwards Turbomolecular Pump) and a coil of heater wire with a cover plate. Temperature measurements were possible as a thermocouple was attached to the cover plate. The wire was heated by means of a DC power supply (voltages 0-30 V, maximum current 5 A). A photograph of this system can be seen in Figure 3.3.

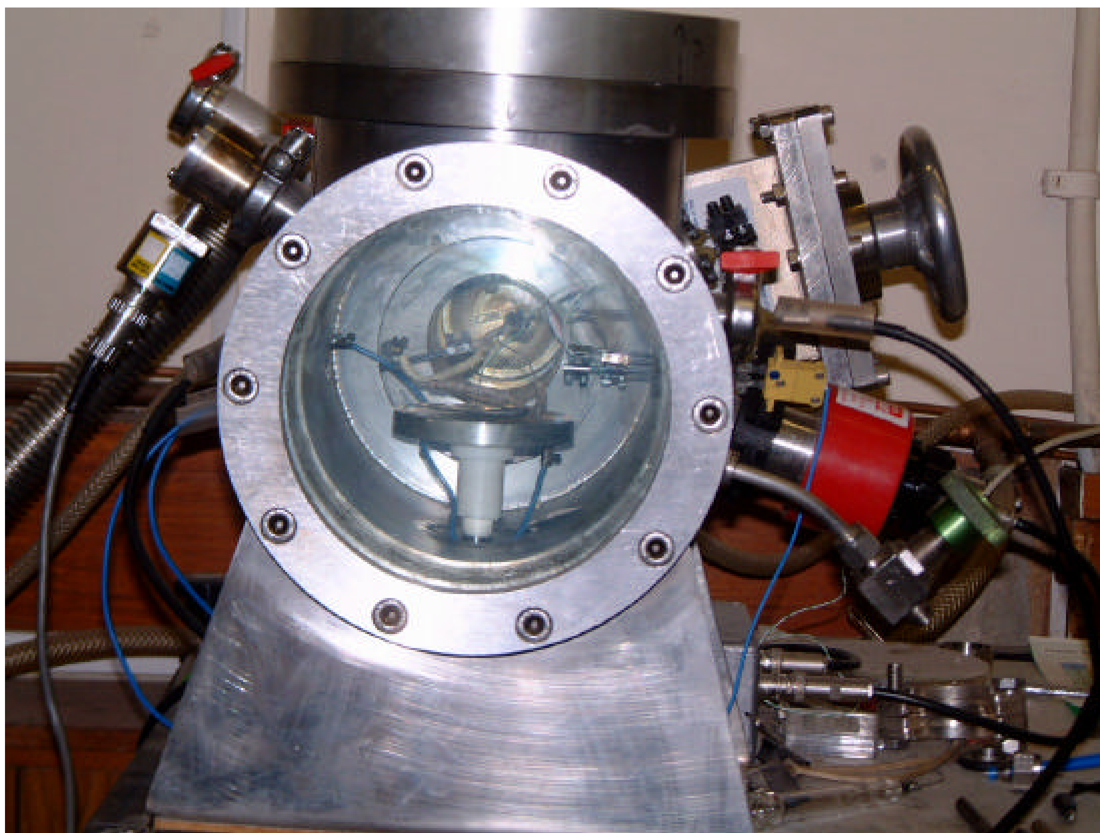

Figure 3.3: Photograph of annealing apparatus.

To use this hotplate, samples were simply placed on the cover plate, the chamber evacuated to a suitable pressure (below 10^{-5} Torr) and the supply turned on and the voltage adjusted until the correct temperature was achieved. The maximum temperature possible with this system was approximately 600 °C.

The system came up to temperature relatively quickly. Temperatures of 400 °C could be obtained in approximately 2 minutes. Temperature decreases were quick until the temperature approached room temperature (100 °C per minute until 200 °C). The temperature could be decreased more quickly if the pressure was increased by venting the chamber with argon.

3.3 Analysis Methods

3.3.1 X-ray Photo-electron Spectroscopy (XPS)

In XPS the sample is placed in the beam of an X-ray source in an Ultra-High Vacuum (UHV) chamber. The X-ray removes core level electrons from the surface of the sample. Ejected electrons from different elements have characteristic kinetic energies. Figure 3.4 shows the mechanism of photoelectron removal.

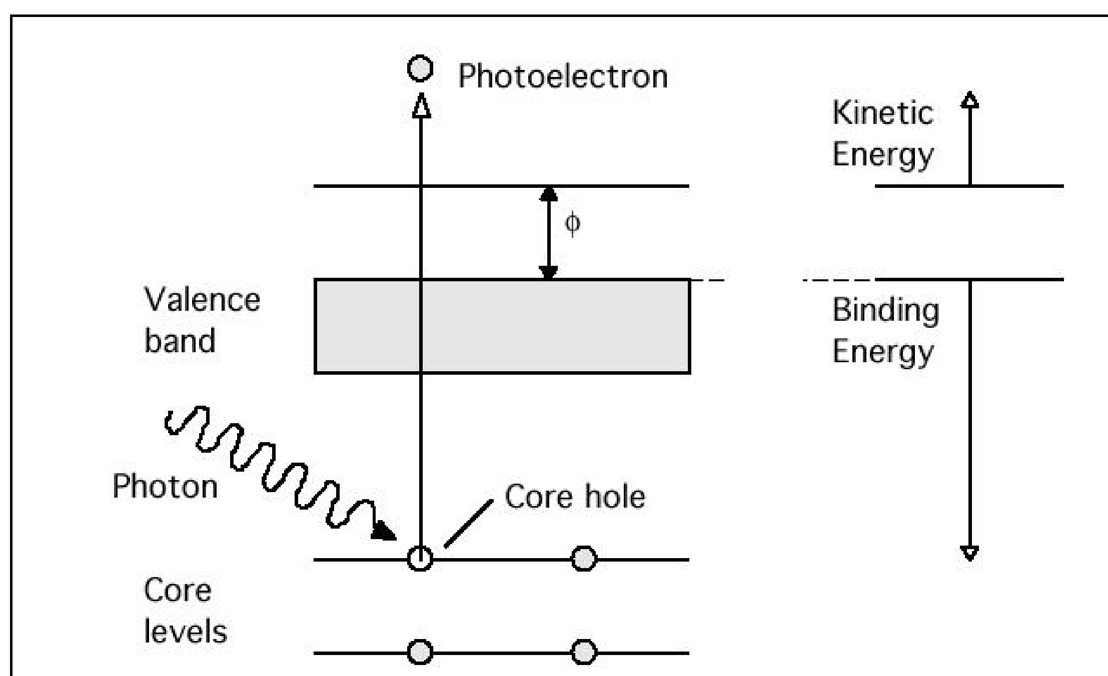

Figure 3.4 The mechanism of photoelectron ejection in X-ray Photoelectron Spectroscopy

The energy of the electrons correspond to Equation 3.1 where E_K is the kinetic energy of the ejected electron, $h\nu$ is the energy of the X-ray source, E_B is the binding energy of the core electron and Φ is the work function of the spectrometer.

$$E_K = h\nu - E_B - \Phi$$

Equation 3.1

It can be seen from Equation 3.1 that an increased binding energy decreases the kinetic energy of the photoelectron. Even though elements have characteristic binding energies, these energies can be changed slightly by the chemical state of the element. Figure 3.5 shows two peaks. These peaks are from a phosphorus 2p spectrum of an oxidised CP thin film. The peak at around 130 eV is from elemental P or P-bound-to-C, the peak at 134 eV is from P-bonded-to-O.

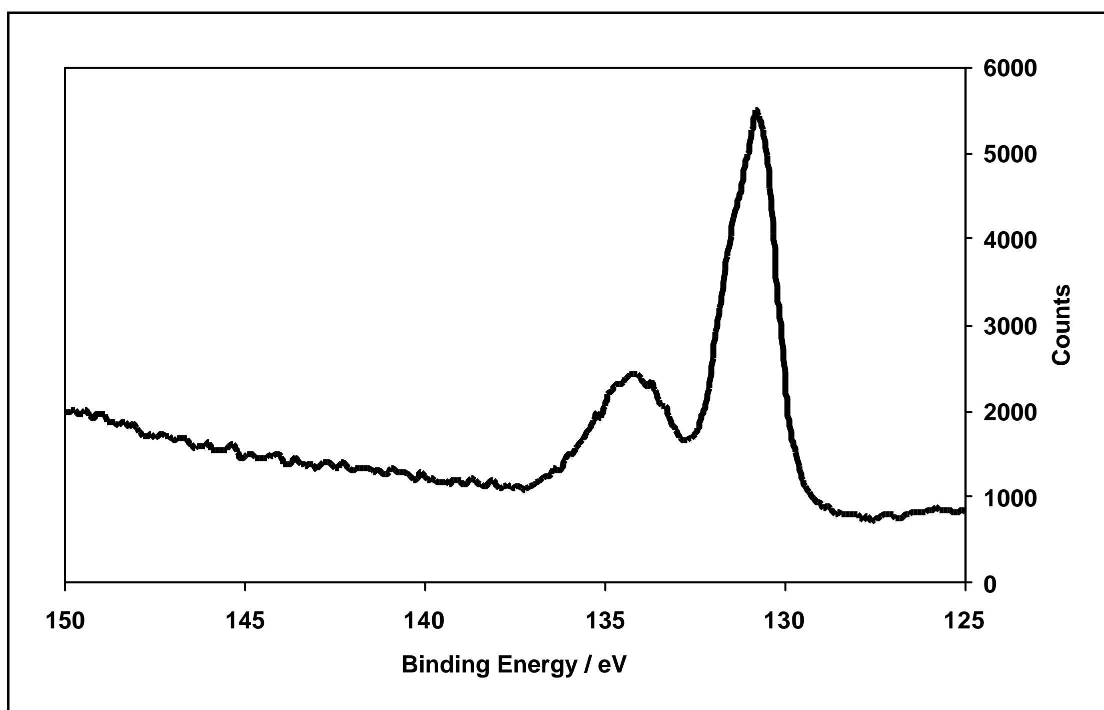

Figure 3.5: A phosphorus 2p X-ray photoelectron spectrum.

The peak shift is not always so dramatic; for example the P-bonded-to-C peak shift cannot even be seen. In these cases curve fitting can be used to quantify different methods of bonding.

In Figure 3.5 there is a slight shoulder on the left hand side of the P 2p peak. This is due to spin orbit coupling. The main peak is from $2p_{3/2}$ electrons and the shoulder

peak is from $2p_{1/2}$ electrons. The magnitude of this splitting increases as Z (the atomic number) increases.

The energies of the photoelectrons are usually measured by a hemispherical energy analyser system, which uses a channeltron (or multiple channeltrons) to detect electrons at different energies. All of the XPS equipment in this study uses a hemispherical energy analyser.

Spectrometers are calibrated to allow accurate quantification of data. The relative sensitivity between elements relative to F is derived empirically [2]. The calibration has been checked against Auger Electron Spectroscopy (AES), these methods agreed to within 2%. The sensitivity factors and information on the line positions of various elements are listed in Reference [3].

The reason that the system must be operated in UHV conditions is that at this pressure few of the electrons collide with any other particle on their way to the energy analyser. XPS is a surface technique. This is because only electrons ejected from atoms close to the surface have any chance of escaping the solid without colliding with another particle. The penetration depth is maximised when the X-ray source and detector are at 90° to each other. Tilting the sample can decrease the penetration depth.

There were two XPS systems used in this study, the most commonly used was a Fisons VG Escascope. The dual anode X-ray source produced either Mg $K\alpha$, or Al $K\alpha$ radiation. Mg $K\alpha$ radiation was always used in this study (1253.60 eV). The

maximum X-ray power used was 450 W. A photograph of the VG Escascope is shown in Figure 3.6.

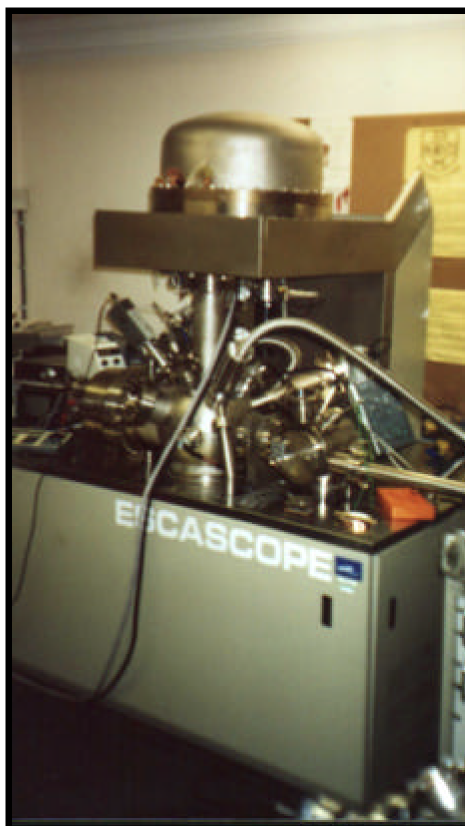

Figure 3.6: A Fisons VG Esascope.

The system consisted of a main chamber with a base pressure of approximately 10^{-10} mbar and an exchange chamber that had a base pressure of around 10^{-7} mbar. A pneumatic gate valve and manipulator arm allowed sample exchange. A turbo pump, backed by a two stage rotary pump, maintained the exchange chamber's vacuum. A titanium sublimation pump and diffusion pump, backed by a two stage rotary pump maintained the main chamber's vacuum.

The diffusion pump oil is known to cause hydrocarbon contamination to the surface of the samples. This was checked by analysis of the same sample several times and

looking at the photoelectron energy line-shape, it was found to have a negligible effect.

The sample stage on this piece of apparatus allowed the loading of multiple samples (a maximum of twelve samples). The computer could then be programmed to run analyses of these multiple samples unattended.

3.3.1.1 X-ray photoelectron spectroscopy at the Daresbury Laboratory Synchrotron Light Source.

The other system was custom built and used at the Daresbury Laboratory in Warrington, Cheshire. The X-ray source was monochromated synchrotron radiation. Synchrotron radiation is generated by the forced change in direction of high-energy electrons; these electrons typically have energy in the region of 5GeV. Electrons are injected into a booster synchrotron and are accelerated by means of an applied radio frequency field. The electrons are then injected into the storage ring. Within the storage ring are a series of bending magnets, these magnets change the path of the electrons and cause radiation to be emitted. This radiation comes off at a tangent to the ring and is passed down a 'beamline'. Within the beamline the beam is collimated and in this specific case is monochromated. At the end of the beamline is the experiment. A schematic of a synchrotron is shown in Figure 3.7. Undulators are also used to boost the flux of the radiation coming from the ring, but these were not used in this study.

The analysis system consisted of a main chamber with a base pressure of 10^{-10} mbar, pumped by a turbomolecular pump and an exchange chamber with a base pressure of

10^{-7} mbar pumped by a turbomolecular pump. Two stage rotary pumps backed both of these chambers.

A manual gate valve and exchange arm allowed exchange of samples. Single samples were transferred on an aluminium plate. This plate was screwed onto an *x, y, z* and θ stage, which allowed manipulation of the sample in the beam. The sample was lined up using visible radiation (blue light) from the synchrotron radiation source. The synchrotron radiation was admitted to the chamber from an aperture, in the side of the chamber.

Radiation was monochromated by a conventional two-circle monochromator that worked by Bragg Diffraction. When the required photon energy was selected the monochromator was moved remotely to obtain the highest signal. A photograph showing the experimental chamber is shown in Figure 3.8. The photon energies used in this study were from 300-700 eV.

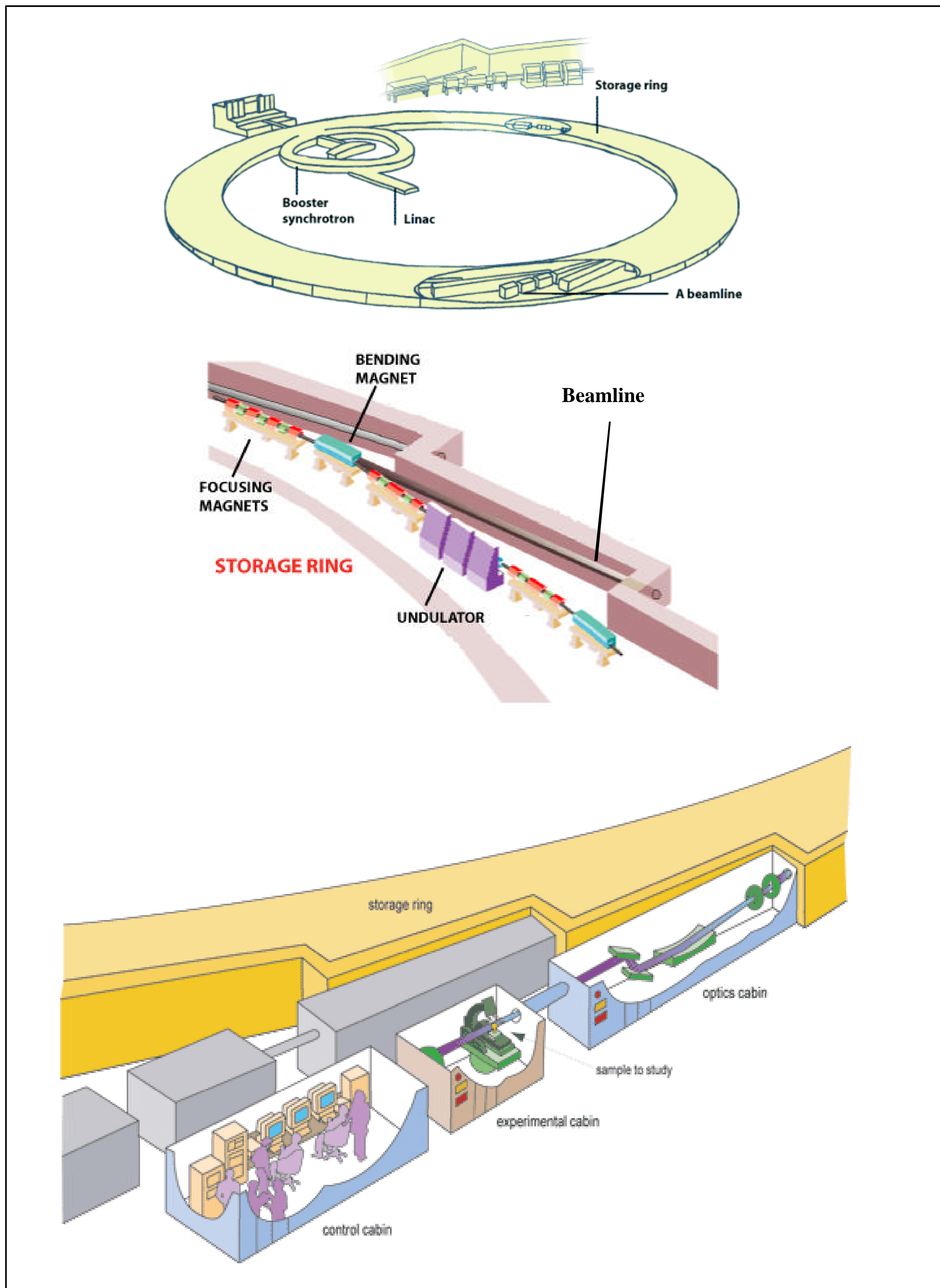

Figure 3.7: A simple schematic diagram of a synchrotron showing the synchrotron, a close up of the storage ring and a typical beamline (top to bottom), these images were taken from http://www.esrf.fr/AboutUs/GuidedTour/printview.

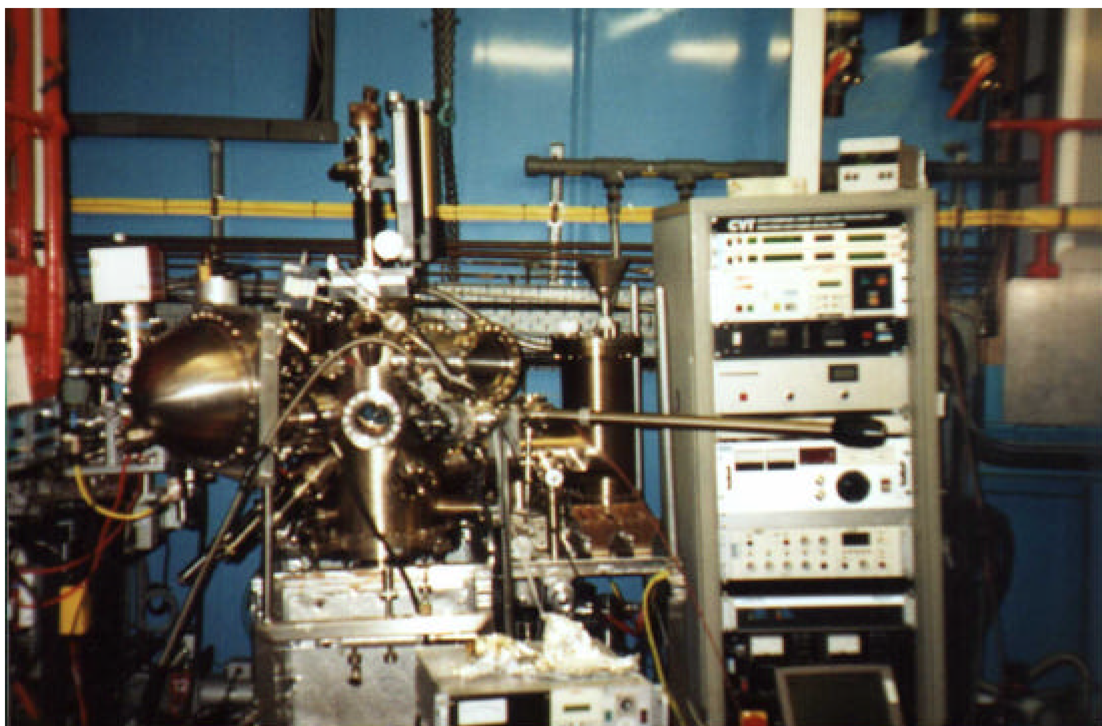

Figure 3.8: The X-ray photoelecton spectrometer used at the Synchrotron Radiation Source, Daresbury, nr Warrington, Cheshire.

The reason for using two different spectrometers was because in any XPS system the full width at half maximum (FWHM) of the peak ($\mathbf{D}E$) is affected as shown in Equation 3.2, where $\mathbf{D}E_N$ is the natural width of the core level, $\mathbf{D}E_P$ is the width of the photon source and $\mathbf{D}E_A$ is the analyser resolution.

$$\Delta E = \sqrt{(\Delta E_N^2 + \Delta E_P^2 + \Delta E_A^2)}$$

Equation 3.2

The natural width of the core level is small, the analyser resolution is typically small, but what increases ΔE most significantly is the photon source width. The minimum FWHM for the VG Escascope is approximately 0.95 eV. It can be seen that having a monochromated source would be beneficial. But conventional monochromator systems have a much lower photon flux. Synchrotron radiation is extremely intense

and when monochromated is still intense. It was thought that it may be useful to use this set-up to fit peaks more accurately.

This was not the case though, as the analyser was not of sufficient quality to improve the FWHM significantly.

3.3.2 Secondary Ion Mass Spectrometry (SIMS)

In SIMS, a focused beam of high-energy ions in a UHV system damages a surface causing surface ions, atoms and molecules to be ejected. The ejected particles' masses are then measured using a mass spectrometer and useful information may be gained about the surface. Figure 3.9 gives an illustration of how SIMS works.

In this study a Ga ion beam is rastered over the sample. The sample is biased at 4kV at the same polarity to the ions that are being studied. This causes the sample to repel the ions. The ions then travel into a mass spectrometer.

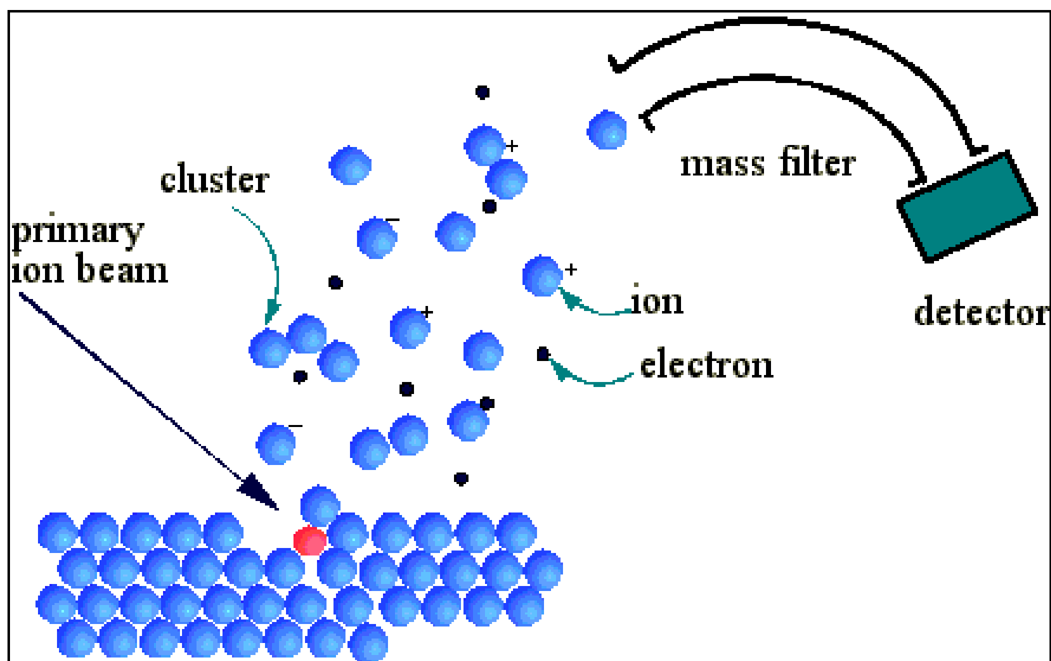

Figure 3.9: A schematic diagram showing the mechanism of ion ejection in SIMS [4].

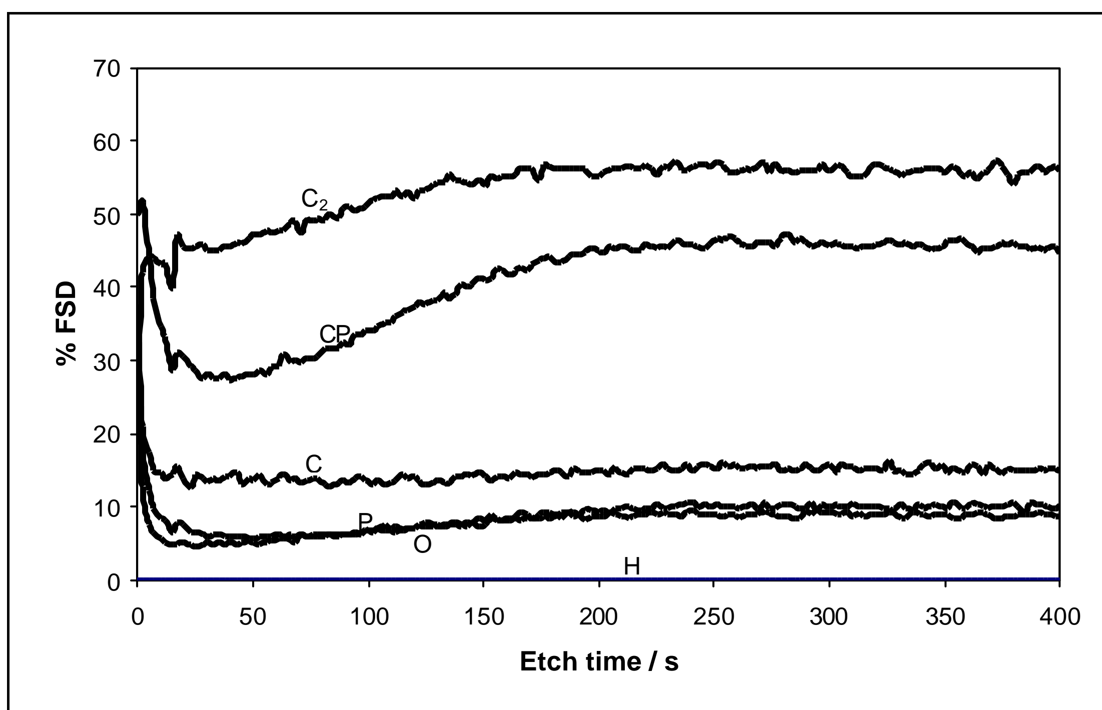

Figure 3.10: SIMS depth profile of a CP thin film.

The ions dislodging surface species cause damage to the sample. If SIMS is carried out over a long time an idea of the depth uniformity of a thin film can be determined.

this technique is called depth profiling. Figure 3.10 shows a typical depth profile of a CP containing film. The units of the x-axis are in seconds. As there are many factors which affect the etch rate of an ion beam, it is only possible to calibrate the x-axis for distance by measuring the film thickness and ensuring that the ion beam is allowed to etch the whole film away. For thicker films and low ion beam currents this can take a very long time (hours or days), so it is usual to express the x-axis in time units.

As well as ions, atoms and molecules the ion beam creates secondary electron emission. This secondary electron emission can be used to visualise the surface of the sample. The image is similar to those obtained by SEM.

In time with the ion beam raster the data collection system can collect mass data. These pieces of data can be fitted together to generate chemical map data. This can show whether chemical species are localised or spread evenly about the surface. Figure 3.11 shows a typical chemical map. The red spot on the centre is a previously etched area so shows chemical data from below the film surface.

The ability of the spectrometer to detect various ions depends on many factors including the stability of the ion, the ionisation energy, or electron affinity of the parent specie and the properties of the solid matrix from which the ion came from. Therefore the sensitivity of the spectrometer may vary by several orders of magnitude. It follows that quantification is difficult.

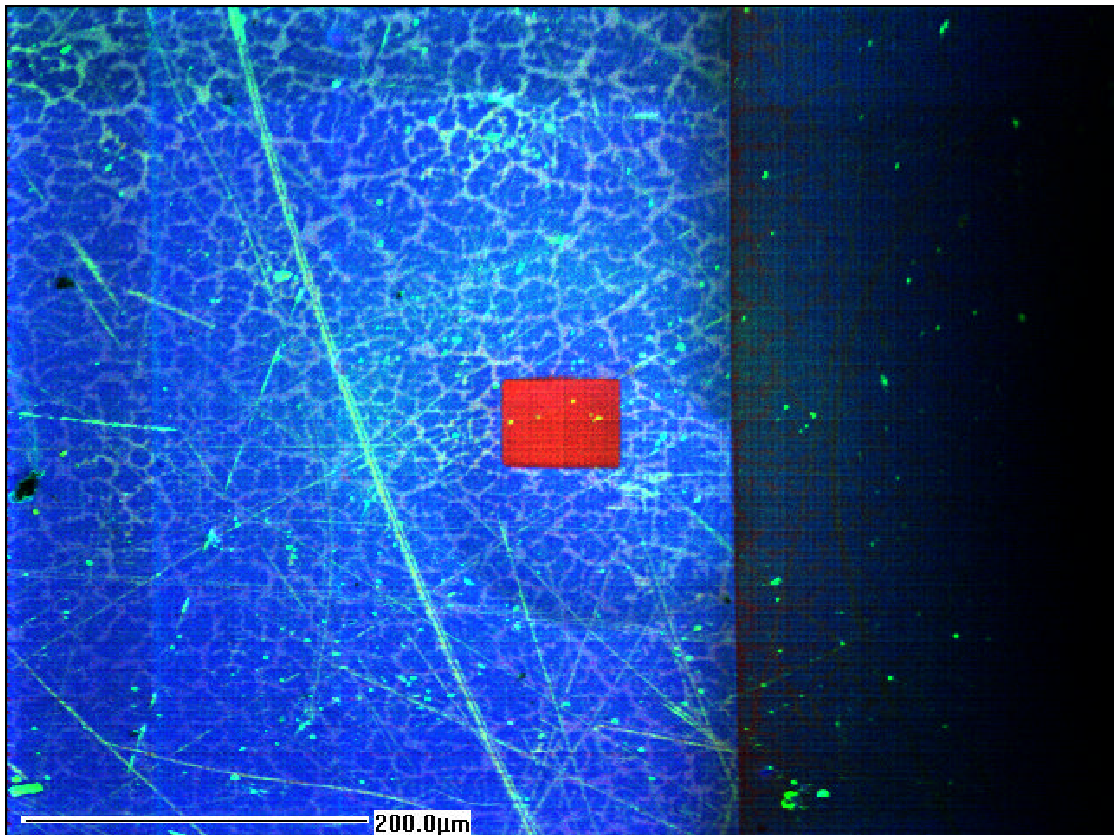

Figure 3.11: Element map overlaid on a secondary electron image of a typical CP film. Red is CP^-, green is O^- and blue is C_2^-.

The system used in this study was custom built by the Interface Analysis Centre.

It had a Ga ion source and a magnetic sector mass spectrometer.

It was used in "negative mode". This meant that only negative ions would be detected. This mode was best to detect the species of interest. The system was also used in "positive mode", but it gave no useful data. This was because all of the parent clusters analysed were more stable as anions than cations. Beam currents of 0.1-10 nA were used in this study.

The focused ion beam (FIB) in this or a similar apparatus can also be used for patterning and etching for device fabrication, TEM sectioning or as used in this study

film thickness measurements. In film thickness measurements a piece of platinum is deposited on top of the study area (usually with a thickness of around 1 µm) to increase the contrast. An etch pit is then made, the sample is tilted and the film thickness is easily measured. An example of this type of film thickness measurement can be seen in Figure 3.12. The apparatus used in this study for FIB determination of the film thickness was a FEI Strata FIB201 system.

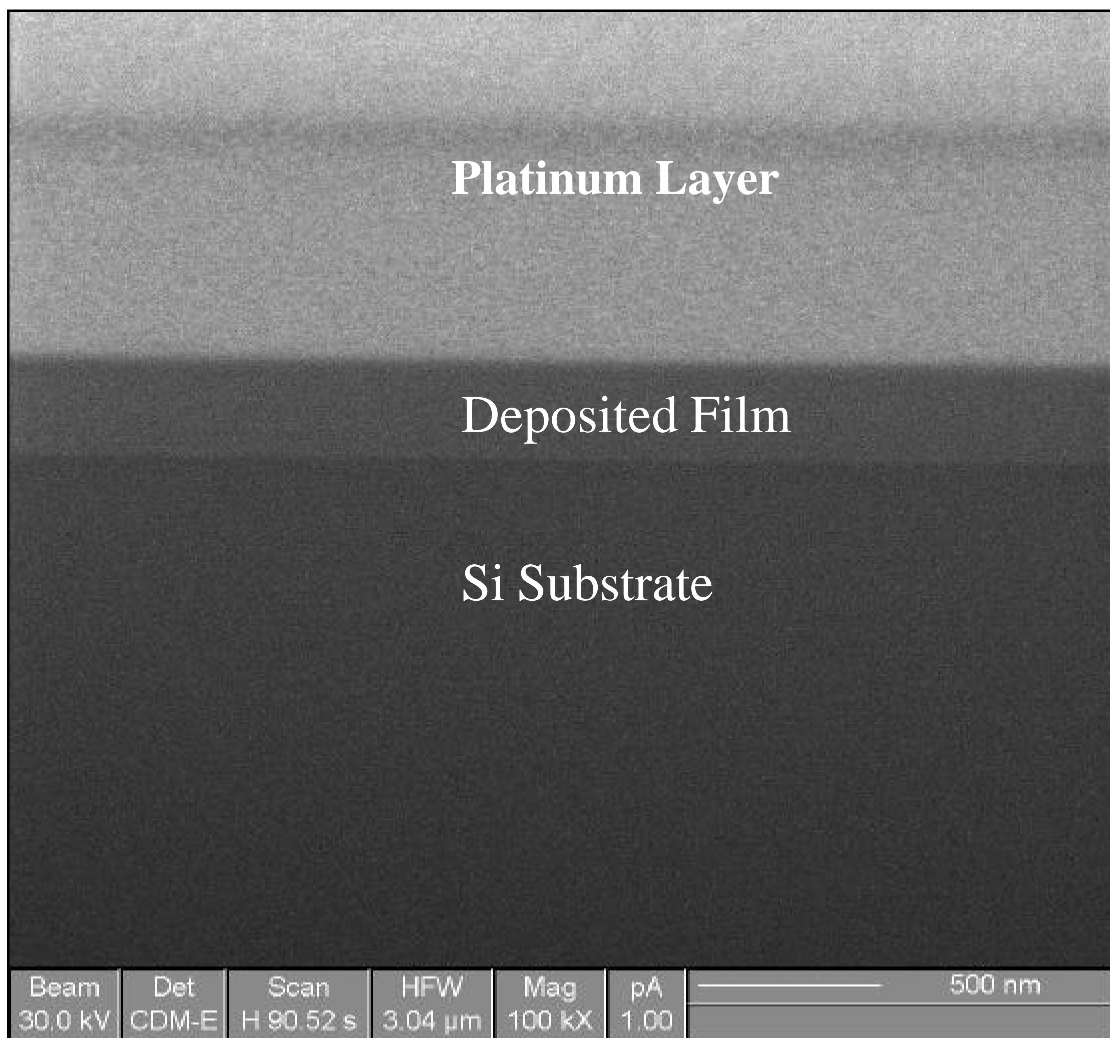

Figure 3.12: An example of how a focused ion beam apparatus may be used to determine the thickness of a thin film.

3.3.3. Auger Electron Spectroscopy (AES) and Energy Dispersive X-ray Spectroscopy (EDX)

AES is a widely used UHV technique for determining the surface composition of a variety of materials. A high-energy primary electron beam is rastered over the sample. This will remove secondary electrons from the atoms that make up the material. These secondary electrons originate from core orbitals. This leaves a vacancy. An electron from a higher lying level drops to this vacant core level. A quantity of energy is released from this transition. This can either take the form of a photon (having very short wavelength), or an Auger electron. This is illustrated in Figure 3.13.

The emission of a photon is used in EDX (also known as X-ray fluorescence). The energies of the photons emitted are characteristic of the parent elements. Therefore if the energy of these photons is determined, elemental data can be found. This is a bulk technique, as X-ray photons can escape more easily than Auger electrons.

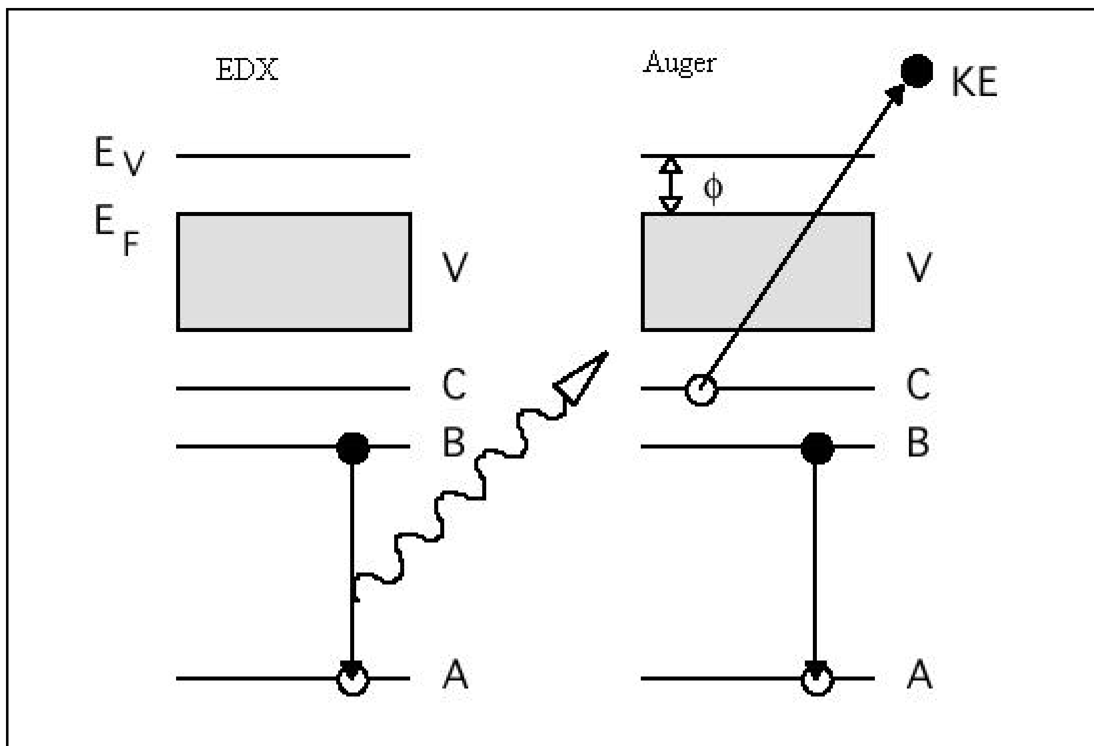

Figure 3.13: The processes involved in the ejection of an Auger electron and an X-ray photon. E_V is the valence band energy, E_F is the fermi level energy, V is the valence level, A, B and C are core levels, f is the work function

Most modern electron microscopes have EDX equipment attached. The disadvantage of this technique is difficult quantification and insensitivity to lighter elements.

All of the EDX data gathered in this study were from various electron microscopes, located in the School of Chemistry and detailed later in the section on electron microscopy.

The energy of the Auger electron is characteristic of the element from which it came. As in XPS it can also be used to give some chemical data. An advantage of this technique is that it has high spatial resolution, but sample analysis is slow.

Nevertheless Auger was used as a technique to check that the sample uniformity was high. Also it was used to check the calibration of the XPS.

The Auger Electron Spectrometer used in this study was a Physical Electronics ϕ595, with a field emission electron source. A photograph of it is shown in Figure 3.14.

Figure 3.14: Photograph of the Auger Electron Spectrometer used in this study

3.3.4 Scanning Electron Microscopy (SEM)

Images in scanning electron microscopy are generated by rastering an electron beam over a sample and collecting the secondary electrons emitted. The resulting image can give information about the uniformity and thickness of the film.

To get film thickness measurements a fresh edge was made by cleaving the film. The film was then mounted "edge up". A simple schematic of an SEM is shown in Figure

3.15. To prevent sample charging samples were sputter coated with a 10 nm platinum film.

Various scanning electron microscopes were used in this study.

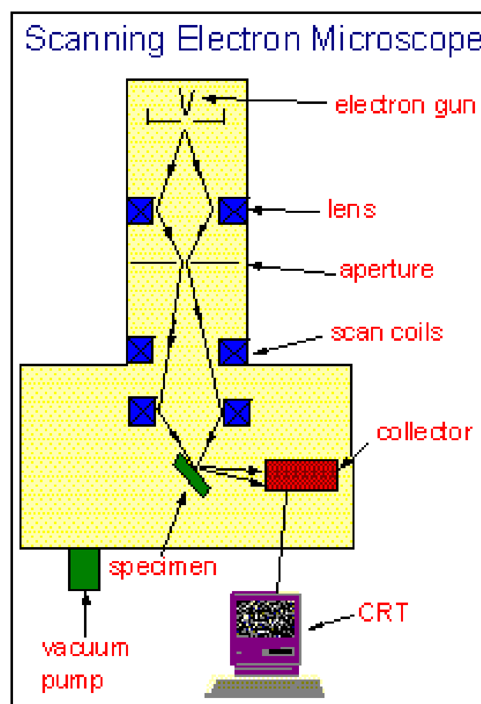

Figure 3.15: A simple schematic of a scanning electron microscope [4].

3.3.5 Transmission Electron Microscopy (TEM)

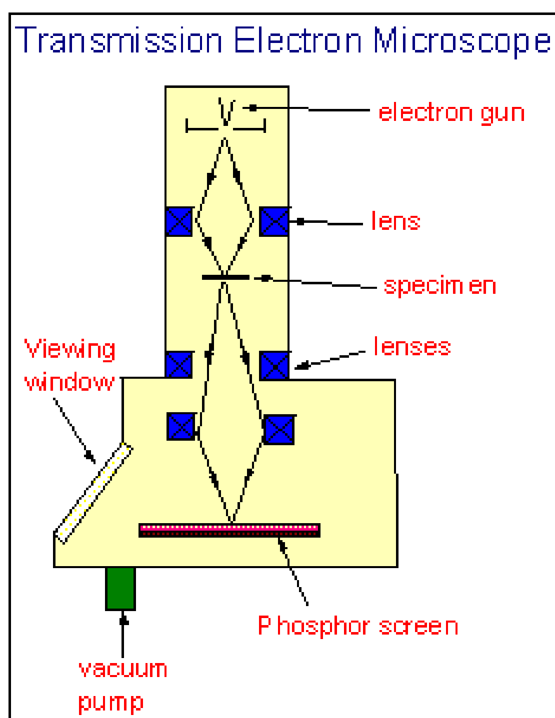

Figure 3.16: A simple schematic of a transmission electron microscope. [4]

In TEM a beam of electrons is spread through several apertures and lenses. This is then passed through the sample and the image focused on a phosphor screen[5]. Generally the electron beam is much more energetic than the beam used in SEM (150-250 kV in TEM compared to 5-30 kV in SEM). This is so that the beam may pass through the sample. This also allows useful crystallographic data to be obtained, which is explained in Equation 3.3 (Bragg's Equation), where λ is the wavelength of the electron, d is the plane spacing of the lattice, θ is the glancing angle.

$$\lambda = 2d \sin \theta$$

Equation 3.3

For plane spacings in the angstrom region, electrons of similar energy (wavelength) are required to obtain useable diffraction angles.

Samples typically have to be a lot thinner (<100 nm) for good images than in SEM. The advantages of TEM are high resolution, easy particle size measurement, the ability to determine crystallinity easily and selected area or nanobeam electron diffraction. This means that very small crystals can be identified and their crystal structures determined relatively easily.

The TEM used in this study was a Jeol 2010, with a 200 kV electron source and a windowless EDX detector (this allowed detection of elements heavier and including C). The microscope was always used at 200 kV. Selected area and nanobeam diffraction patterns were always taken with camera lengths of 80-120 cm.

TEM samples were prepared by dropping the suspension of the sample onto a carbon or SiO coated grid and allowing the solvent to evaporate.

3.3.6 Laser Raman Spectroscopy (LRS)

When a laser is focused on a sample most of the light is reflected straight back. This is called elastic scattering or Rayleigh scattering. The film may absorb a small amount of the light. This absorption will produce an excited state. In a solid this will be a vibrationally excited state. This vibration will be set up on a large scale in the bulk (the whole localised structure vibrating). This is called a phonon vibration.

The photon re-emitted from this state will have a lower energy than the incident photon; this light is called Stokes radiation. If a photon is absorbed onto a molecule which is already excited the photon emitted will have a higher energy than the

incident photon. This light is called anti-Stokes radiation. The technique that measures the emission of Stokes and anti-Stokes radiation is called Raman Spectroscopy[6].

In the system used in this study, a laser is passed into the spectrometer and directed into the microscope by a series of mirrors. The laser is then focused onto the surface of the sample. Light reflects off the sample. This Rayleigh radiation is filtered out at the holographic notch filter. The light is put through a lens and a slit to filter the light. The light is then passed through another lens, onto a mirror and then onto a grating. The light is then captured on a CCD array. The computer then interprets the CCD information and displays a spectrum. A diagram of the laser Raman spectrometer used in this study is given in Figure 3.17.

The laser Raman spectrometer used in this study was a Renishaw 2000 multi laser Raman spectrometer. It used a 785 nm diode laser, a 514 nm Ar ion laser and a 325 nm Cd vapour laser. Early Raman measurements were taken on a Renishaw 2000 Raman spectrometer with a 488 nm laser.

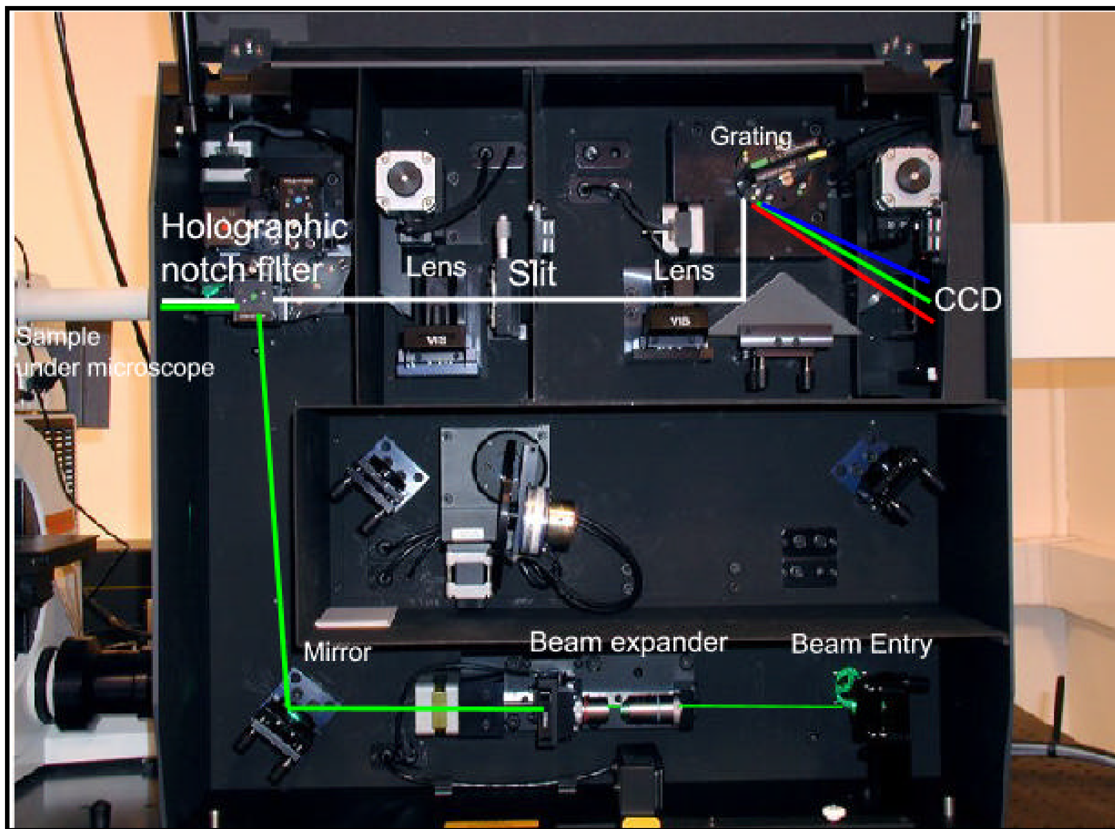

Figure 3.17: Laser Raman Spectrometer with drawn guide lines to show how light is passed through the spectrometer.

3.3.7 Ultraviolet / visible (UV/Vis) spectroscopy

In UV/Vis spectroscopy a light source is shone through a sample and the absorption measured. The absorptions are due to electronic transitions in the sample. In thin film samples the optical band gap (E_g) can be estimated by extrapolating from the linear part of the absorption spectrum. The point at which the line intersects with the energy axis corresponds to the approximate optical band gap of the material. This method is a Tauc type plot[7]. Figure 3.18 shows a Tauc type plot, estimating the optical band gap of a thin film.

All films that were analysed by UV/Vis were deposited onto quartz substrates, so that the light from the spectrometer would pass through the sample.

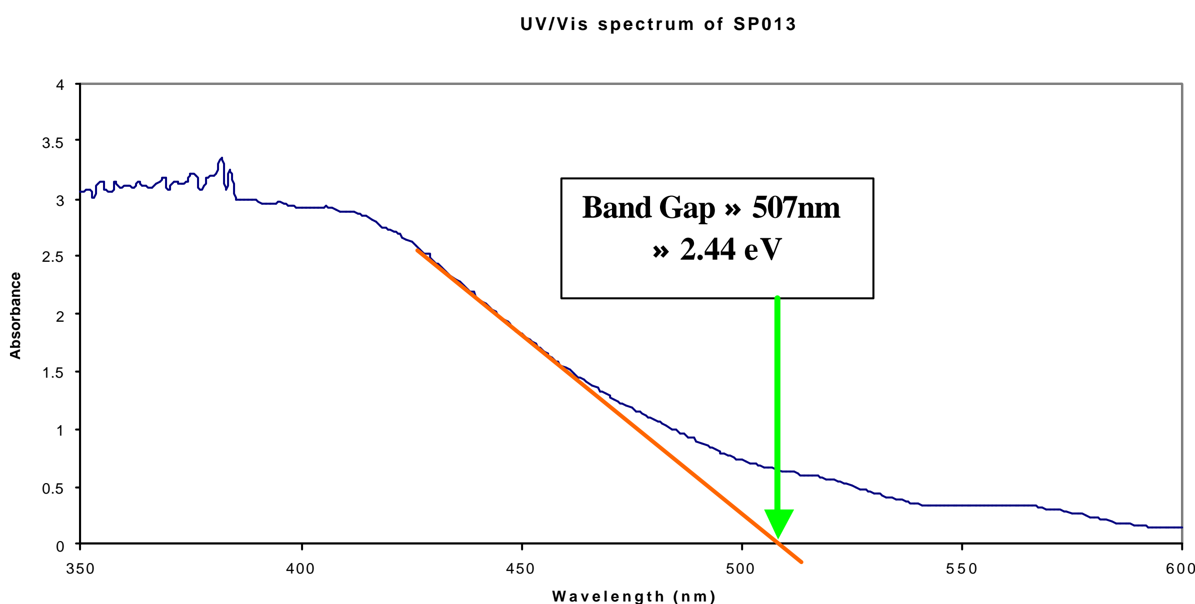

Figure 3.18: A Tauc type plot estimating the optical band gap of a thin film

3.3.8 Optical Emission Spectroscopy (OES)

During deposition using both the RFCVD and PLD methods light is emitted from species that are present within the plasma. Light from different emitting species can be identified using various references[8]. This gives a quick and easy way of identifying some of the species present in plasma under different conditions.

It is important to note that only some species emit light in the plasma, so this technique does not give an exhaustive list of what is present. It is also worth noting that only a small proportion of any given species will emit. Therefore it is difficult to determine relative concentrations of species.

The light from the RF deposition plasma was captured via a telescope with a focal length of 20 cm (which was focused onto the plasma). This was passed via a grating

to a charge-coupled device (CCD) via a quartz fibre optic bundle. The system used was an Oriel Instaspec IV, the monochromator had a 600 lines/mm grating and had a resolution of 0.9 nm.

When the light emission from the plasma from RF-CVD was being measured the telescope was focused into the chamber via the quartz window. For the laser ablation the telescope was pointed at the plasma, but because the plasma existed as a pulse, the laser and spectrometer were computer triggered. They were set up so that the spectrometer recorded light at the instant that the laser was fired and for 0.1 seconds after. It did this for several hundred laser shots and accumulated the data.

Calibration of the spectrometer was carried out by focusing the spectrometer onto Hg strip lights (several emission wavelengths were used depending on the range of the OES measurement).

3.3.9 X-ray Powder Diffraction (XRD)

The crystallinity of CVD samples was checked by XRD. In this method, X-rays are shone at the sample at varying angles. The detector travels at a varying angle and detects diffracted X-rays. A photograph of the apparatus is shown in Figure 3.19. The XRD equipment used in this study was a Bruker-Nonius D8 Powder Diffractometer. The X-ray source was Cu, with a photon energy of 8 keV.

The Bragg equation (equation 3.3) shows that the lattice spacings may be found from the diffraction angle.

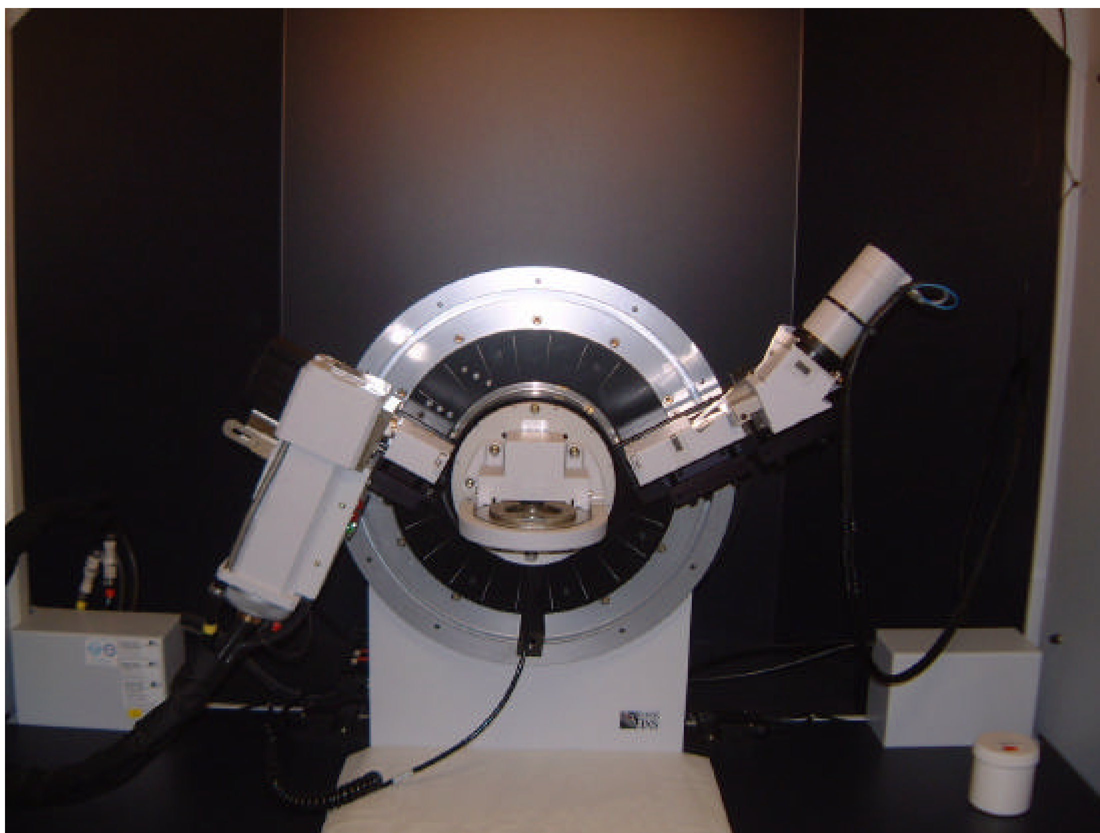

Figure 3.19: Photograph of the X-ray powder Diffractometer used in this study, the X-ray source is on the left, the sample is in the middle and the detector is on the right.

3.4 References

1 M. T. Kuo, P. W. May, A. Gunn, M. N. R. Ashfold and R. K. Wild, Diamond and Related Materials **9,** 1222-1227 (2000).

2 C. D. Wagner, L. E. Davis, M. V. Zeller, J. A. Taylor, R. H. Raymond and L. H. Gale, Surf. Interface Anal. **3** (1981).

3 *Handbook of X-ray Photoelectron Spectrscopy* (Perkin-Elmer Corp, 1992).

4 P. W. May. BSc Surface Science Course handout 2000

5 B. Fultz and J. M. Howe, *Transmission Electron Microscopy and Diffractometry of Materials* (Springer, 2000).

6 H. Baranska, A. Labudsinska and J. Terpinski, *Laser Raman Spectrometry Analytical Applications* (1987).

7 J. Tauc, *Optical Properties of Solids* (1972).

8 R. W. B. Pearse and A. G. Gaydon, *The Identification of Molecular Spectra*, fourth ed. (John Wiley & Sons, Inc, 1976).